

A study and measurement of the behavior of asymmetric samples, in neutron-graphy, using Monte-Carlo simulation

K Kamali Moghadam and H Afarideh

Nuclear Research Center, Atomic Energy Organization of Iran, P. O. Box 11365-8486,
Tehran, Iran

Received 9 July 1993, accepted 11 August 1994

Abstract : Recently in the wake of neutron radiography research, we developed and mobilized the 5 MW reactor of the Nuclear Research Center of Tehran with installing new equipment

By using Gd foil and (LiF-ZnS) neutron converters, a set of radiographic images were recorded from each sample. Each image was obtained through successive rotations in steps of 1.8 degrees, spanning from 0–180 degrees, about axes perpendicular to the direction of the incident beam. The data on each film was read by an optical densitometer and later transferred to a PC for further analysis. To construct a picture or a tomogram of a slice, computer programs based on various mathematical techniques such as "Filtered Back Projection", were developed and used.

The main problem in the analysis process was the contribution of the scattered neutrons to the incident ones. This problem magnifies itself for asymmetric samples and could cause a more disturbed image, due to non-uniform contribution of scattered neutrons. A program based on Monte-Carlo method was developed and used to resolve this problem and the results are presented.

Keywords : Neutron radiography, non-destructive testing, Monte-Carlo method, computed tomography

PACS Nos. : 81.70.Dw, 87.59.Fm, 02.70.Lq

1. Introduction

Neutron radiography as a Non-Destructive Testing (NDT) technique has been recognized for many years [1,2].

The development of different kinds of neutron sources as well as neutron generators and accelerators along with high-technology-fast-computers, have led to a rapid growth in the field of neutron radiography such as neutron computed tomography. Recently, the use of

non-metallic materials such as carbon epoxy composites and ceramic compounds, have become very common in aerospace and military industries. To examine such materials, neutron radiography is preferred over the X-ray method. Moreover, application of neutron radiography for testing fuel rods in nuclear industries has become a valuable technique [3-5].

In conventional neutron radiography, by passing uniform and parallel beam of neutrons through a sample, it is possible to record its internal structure on a film. In this way, the internal structure of one part of the sample may mask another. Thus, obtaining the definition of a random structure becomes difficult and sometimes impossible. To overcome this difficulty, Neutron Computed Tomography could be employed to produce an image from a thin layer of the sample without any interference. To perform this, the object should be rotated in equal angles around a fixed axes perpendicular to the slice. Afterwards, the transmitted neutrons could be recorded by one of the known detecting techniques such as film-converter (Static Method) or TV Camera (Real Time Method).

Exploiting one of the mathematical methods in image reconstruction such as Two Dimensional Fourier method or Filtered Back Projection method, enable us to obtain a tomogram (reconstructed image) of the sample [6-8].

As mentioned earlier, the major problem to obtain a tomogram of a sample is the contribution of the unwanted scattered neutrons. In what follows, we offer a procedure to discount the effect of the unwanted scattered neutron and discriminate them from the main stream of the transmitted neutrons for obtaining a better tomogram.

2. Instrumentation

The present neutron radiography system installed in 5 MW Research Reactor had been designed and constructed over the past several years [9]. The specifications of the system in 1 MW reactor power are as follows :

A neutron flux seen by the sample is about 5×10^4 n/cm²/sec, the cadmium ratio is 20 and the neutron to gamma ratio is 5×10^5 n/cm²/mR.

3. Experimental procedure

To perform computed tomography studies, the equipment designed as well as the programs used in the experiment were as follows :

- A remote-controlled elevator, designed for an automatic replacement of sample, cassettes, films and converters.
- A remote-controlled stepper motor used for rotation of the sample.
- A BF3 neutron detector sensor placed inside the shielding compartment to indicate the neutron flux level. In addition, a set of flashing lights were used as a beam-port-open indicator.

A study and measurement of the behavior of asymmetric samples etc.

Plate I

Figure 1. Example of TOMOG printout, which shows simulation of a hypothetical samples having different density zones. The projection data used for this simulation were obtained by Shepp & Logan method

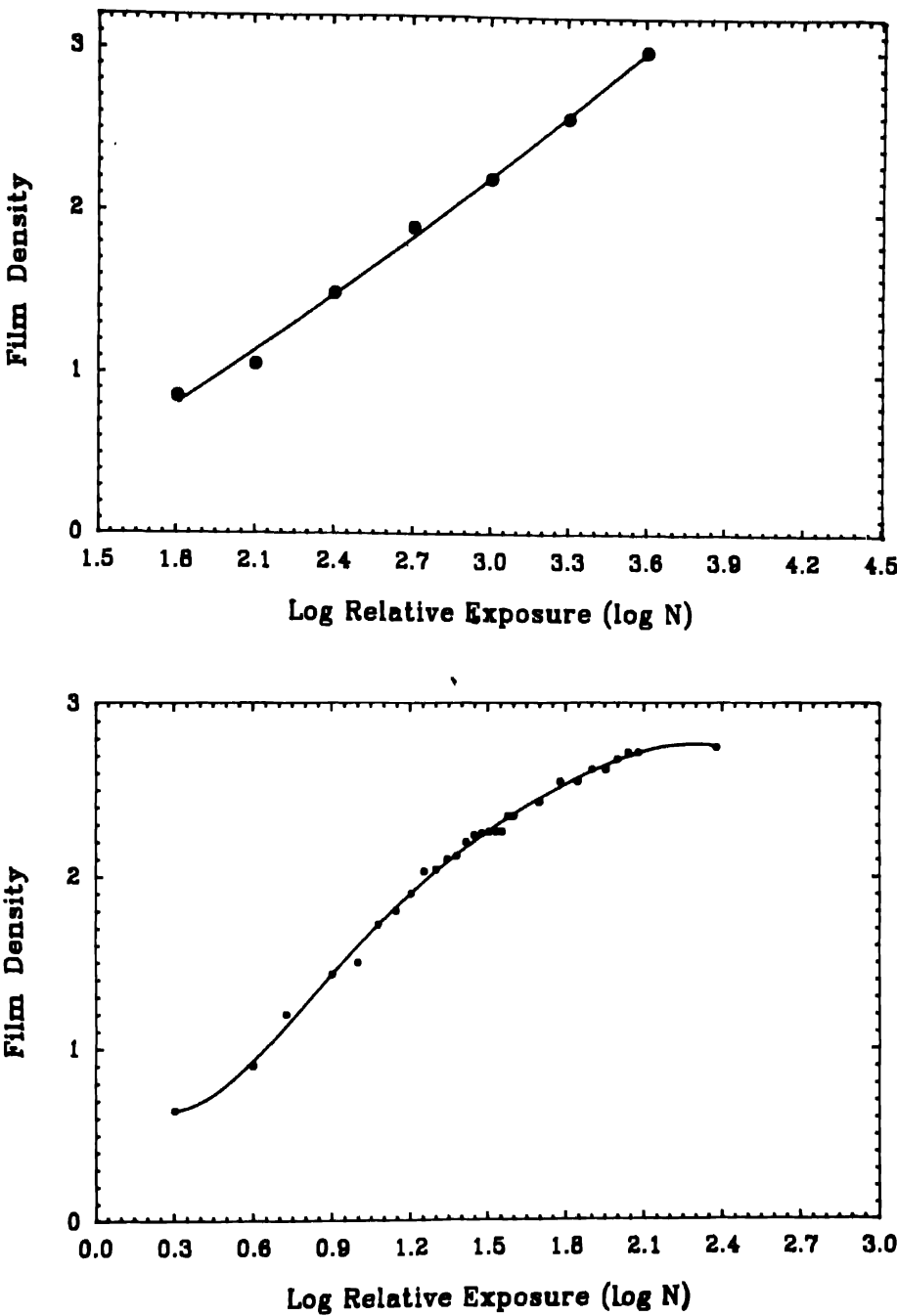


Figure 2. Characteristic curves of the films used in the experiment

BAKPRO – This program computes the total macroscopic cross section distribution of each pixel through the chosen layer or slice of the sample, using Filtered Back Projection method. The projection data could be generated by the program MONT, or by reading off the films as an input data file for this program.

MONT — This program based on Monte-Carlo method is developed to simulate neutron radiography to generate projection data. It computes the probability distribution function of the scattered and transmitted neutrons. The neutron source was assumed to be at infinity so that only parallel beam enter into the object. The object as a phantom sample was assumed to be cylindrical shape with an infinite height and another semi-axes cylindrical material inside it. To execute the program appropriately, information such as dimensions, densities, cross sections, *etc.* for the materials used should be provided as an input data.

TOMOG — This program demonstrates the tomogram or reconstructed image of the sample in two different ways: First, through the PC monitor, using color as grey level monitor and second, through the printout, using dots as grey level monitor. The output data of BAKPRO is used as an input data of this program. Figure 1 shows the printout of a tomogram, using the method of Shepp and Logan [10].

FILM – This program computes the projection data $[\ln(N_0/N)]$. The predetermined characteristic curves as well as the film optical densities obtained by an optical densitometer are used as an input data file. These characteristic curves are presented in Figure 2 [11]. This program also generates correction factors which normalize the input data. The output file consist of the projection data $[\ln(N_0/N)]$ where N and N_0 are the relative exposures of the films with and without the sample.

Under the procedure mentioned above, a Gadolinium (Gd) foil and (LiF-ZnS) scintillator as neutron converters were used with CRT7 (3M) and Mi-Nc (Fuji) films, respectively.

4. Results and discussion

Consulting the macroscopic neutron scattering cross section data, one finds that values are mostly around 0.5 cm^{-1} as shown in Figure 3.

In this respect, we decided to study the scattering in the absence of the absorption. Then attempts were made to investigate the effect of the absorption on scattered neutrons distribution inside and outside of the sample, having neutron scattering cross section equal to 0.5 cm^{-1} . A phantom of cylindrical shape, 4 cm in diameter, was used for experimental and computational work. For asymmetric situations this phantom assumed to be made of Al with another cylindrical material, like H_2O , CH_2 and Cu with 1 cm in diameter. The axes of both cylinders are assumed to be parallel and 1 cm apart (see Figure 4). The phantom should

consist of materials in which the ratio of the transmitted neutrons to the incident ones be more than 3%. This value corresponds to the linear part of the film characteristic curves (see Figure 3). In this respect, the phantom used for this experiment found to be quite suitable.

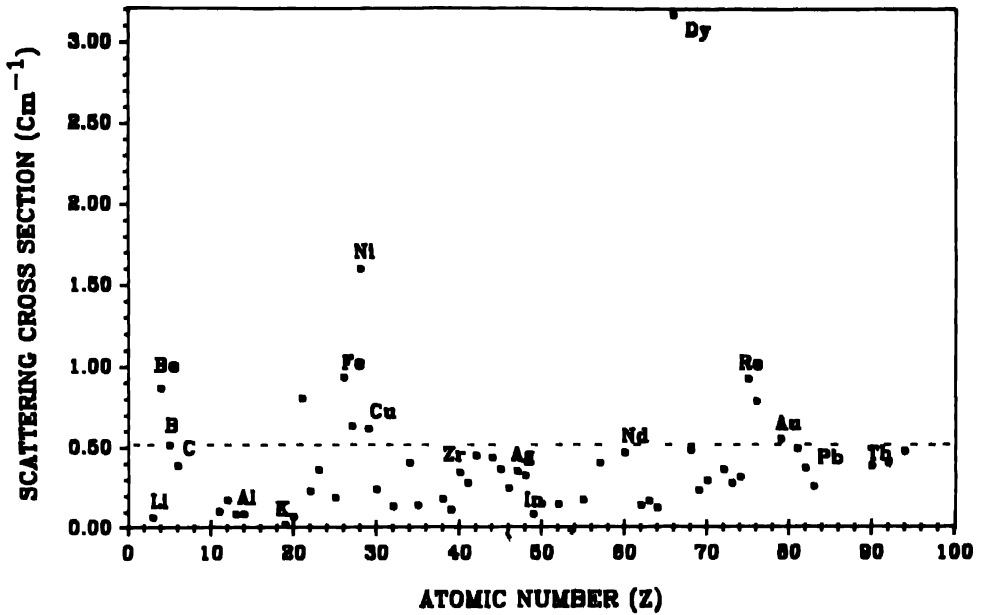


Figure 3. Macroscopic neutron scattering cross-section distributions of the elements

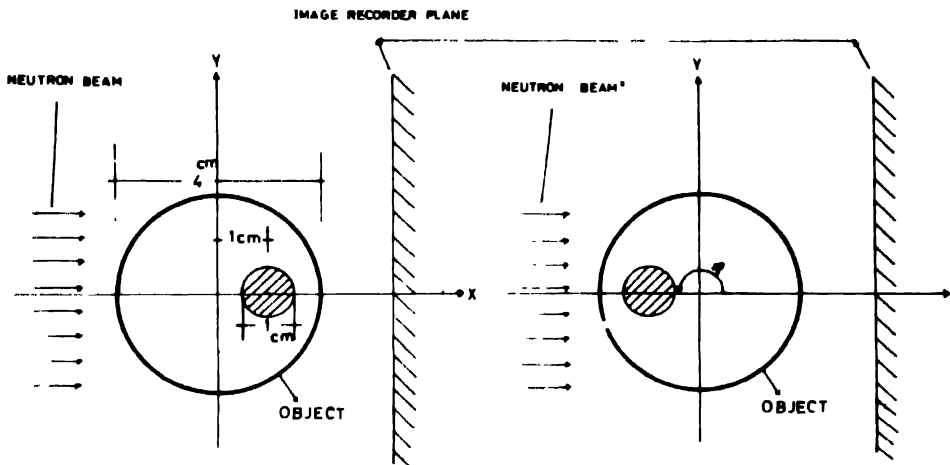


Figure 4. Top view cross-section of chosen phantom.

The effect of scattered neutrons on transmitted neutrons through cylindrical shape material, is called scattering probability distribution per pixel. In Figures 5a and 5b, the effect of scattering in zero absorption cross section materials are demonstrated. The results for

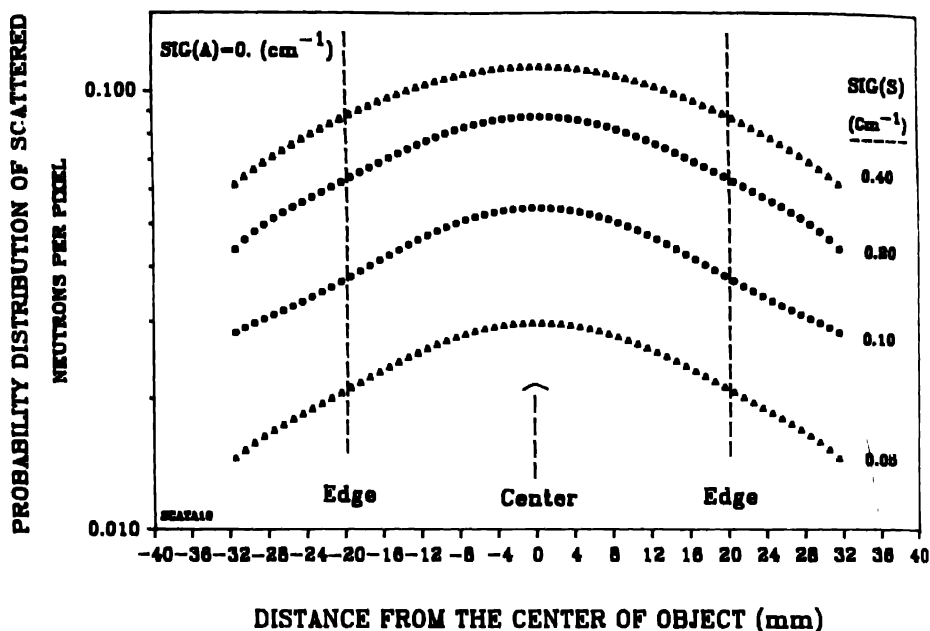


Figure 5a. Shows the scattered neutron probability distribution, re-entering into the initial beam, for a hypothetical object having zero macroscopic absorption cross-section, and its macroscopic scattering cross-section varying between 0.05 and 0.4 cm^{-1}

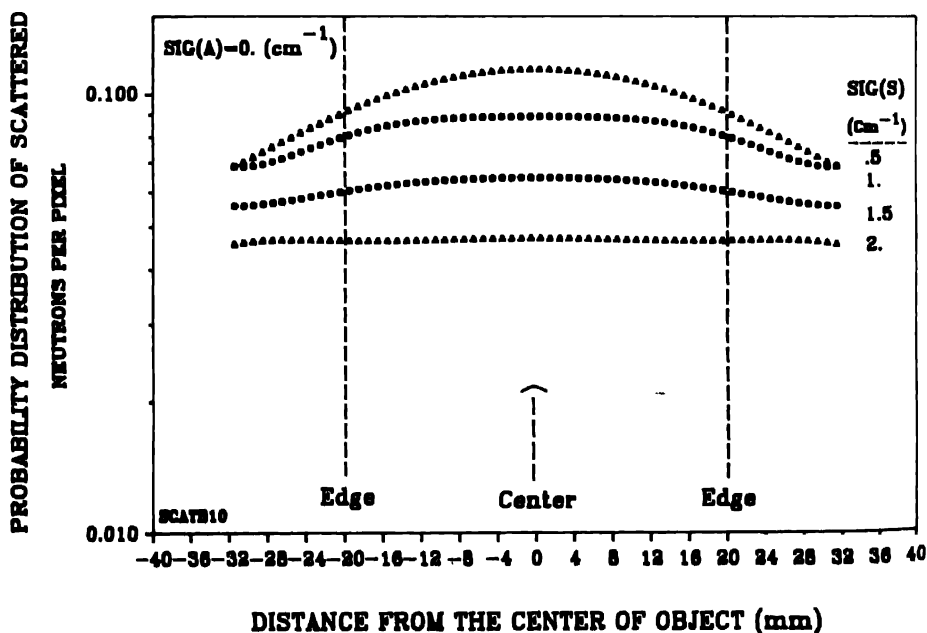


Figure 5b. Is the same as Figure 5a, but for macroscopic scattering cross-section varying between 0.5 and 2 cm^{-1} .

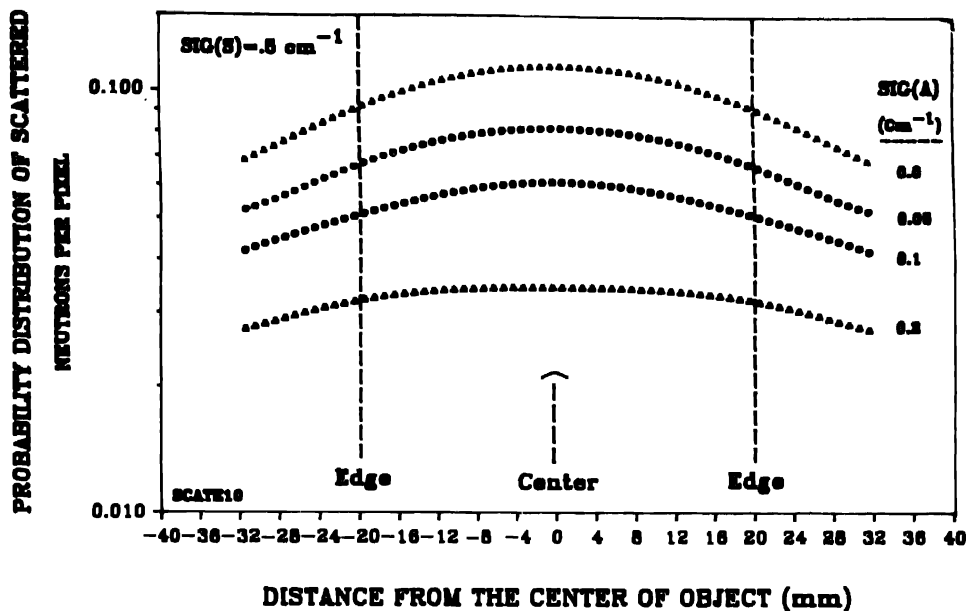


Figure 6a. Shows similar curves as in Figure 5, where macroscopic scattering cross-section is $0.5 cm^{-1}$ and macroscopic absorption cross-section varying between 0.05 and $0.2 cm^{-1}$.

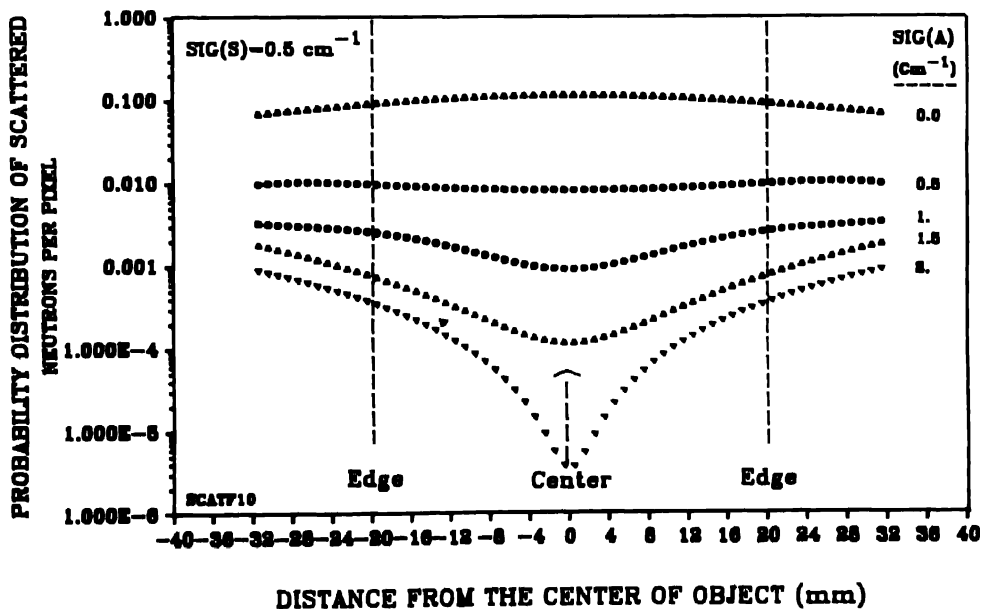


Figure 6b. Is the same as Figure 6a, but for macroscopic absorption cross-section varying between 0.5 and $2 cm^{-1}$

hypothetical materials with fixed scattering cross section of 0.5 cm^{-1} and varying absorption cross section are illustrated in Figures 6a and 6b. The results obtained for asymmetrical

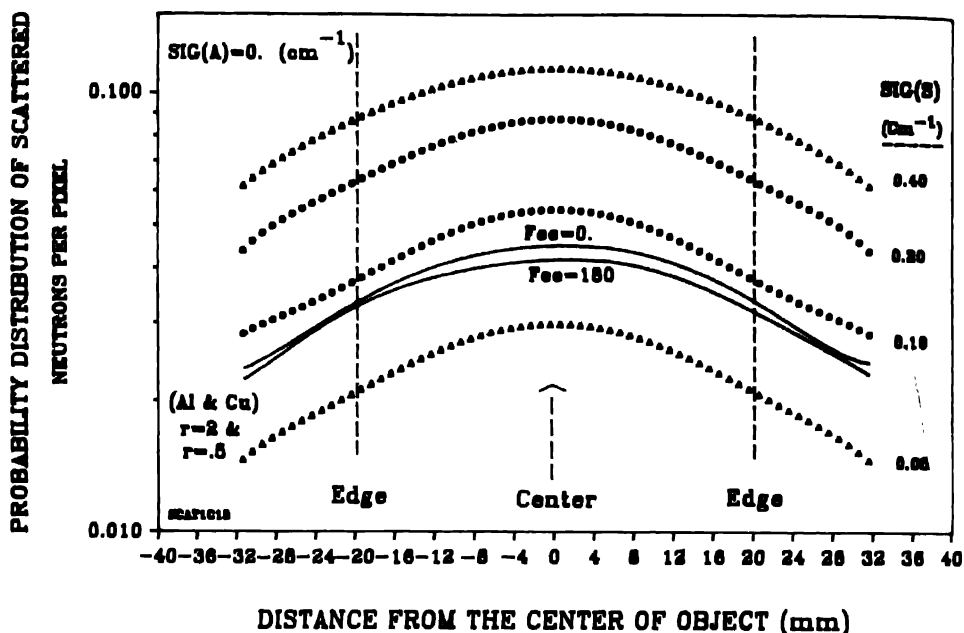


Figure 7. Shows the scattered neutron probability distribution, re-entering into the initial beam, for asymmetric object consisting of two cylinders of Al and Cu, where their axes located one centimeter apart. Al and Cu cylinders having 2 and 0.5 cm in radius, respectively. The angle between the direction of the incident beam and a line joining the center of these cylinders are 0 and 180 degrees

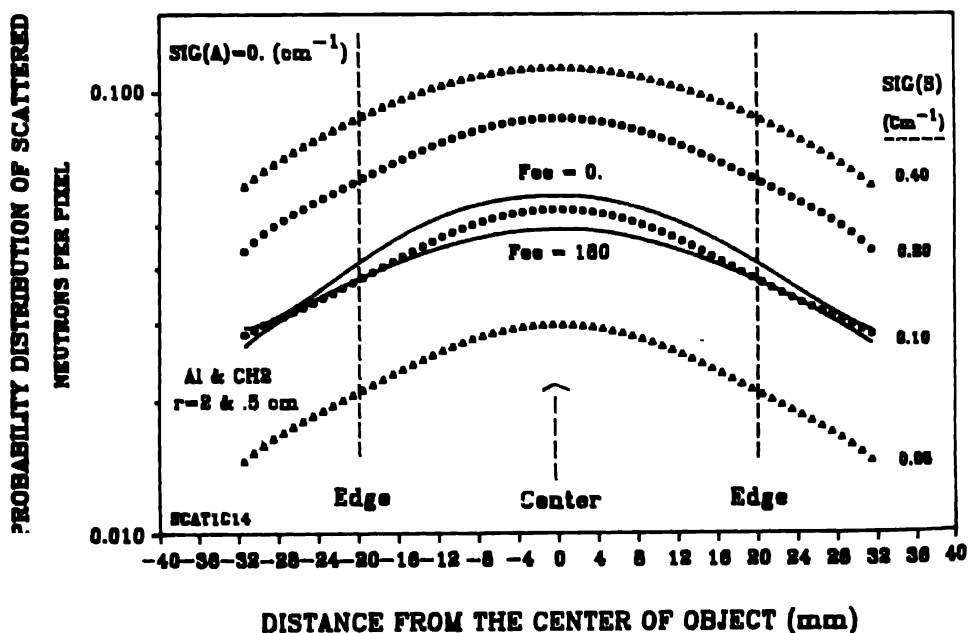


Figure 8. The same as Figure 7 except $(\text{CH}_2)_n$ replace Cu.

situation as mentioned above for Al-H₂O, Al-CH₂ and Al-Cu are illustrated by solid curves in Figures 7, 8 and 9, respectively. In order to explain the effect of absorption, information of Figure 5a for comparison is also included in these figures. We chose only compound materials such as water (H₂O) and polyethylene [(CH₂)_n] as well as aluminium (Al) and copper (Cu) elements due to their applications in nuclear industry. Moreover, the compound materials of polyethylene and water being light elements are quite suitable for the study of scattering phenomenon. Likewise, aluminium is preferred for its small absorption and scattering.

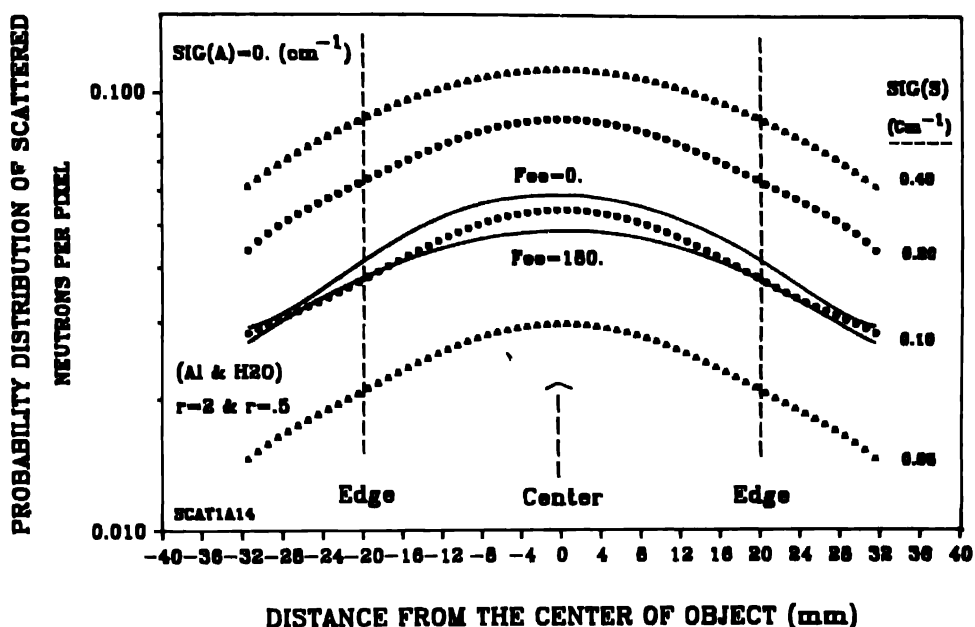


Figure 9. The same as Figure 7 except H₂O replace Cu

For a symmetrical object the comparison of $\ln(N_o/N)$ for the two different arrangements of Al-Cu-Al and Cu-Al-Cu sandwiched in three consecutive coaxial cylinders is shown in Figure 10a. Meanwhile, the comparison of neutron distribution distortions for the two arrangement mentioned above is shown in Figure 10b.

5. Conclusion and suggestions

In the absence of neutron absorption for a symmetrical object the distribution of the scattered neutrons is expected to be Gaussian, since the scattering is a statistical phenomenon. The curves in Figure 6 clearly indicate that, increasing the value of neutron absorption of samples will cause the probability distribution curves deviate from Gaussian. For macroscopic absorption cross section ($\Sigma\alpha$) around 0.5 cm⁻¹, the scattered neutron distribution becomes uniform. Higher values of $\Sigma\alpha$ would result in lower values of the probability distribution in

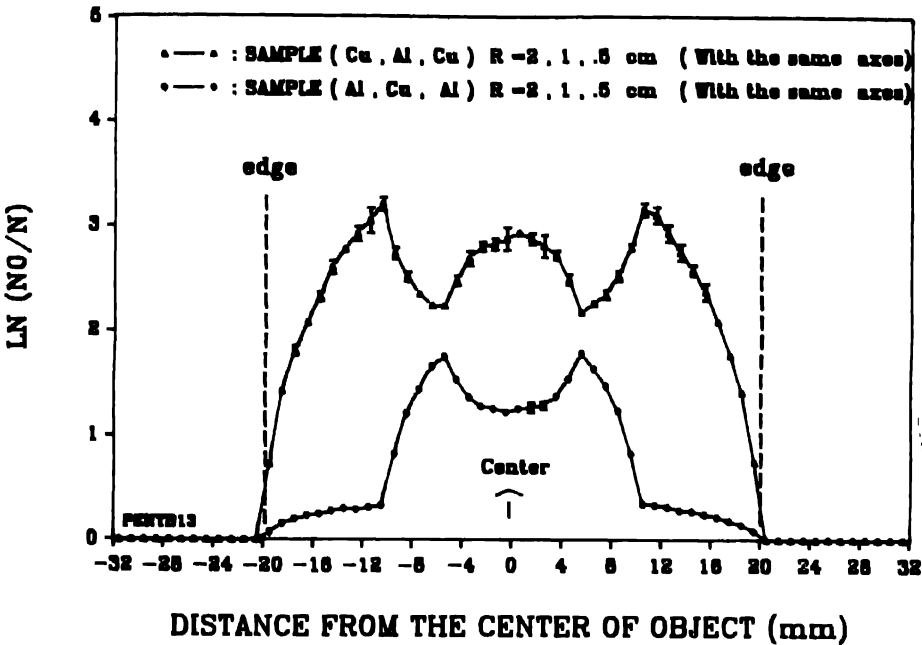


Figure 10a. Presents the projection data for the two arrangement of Cu-Al-Cu and Al-Cu-Al

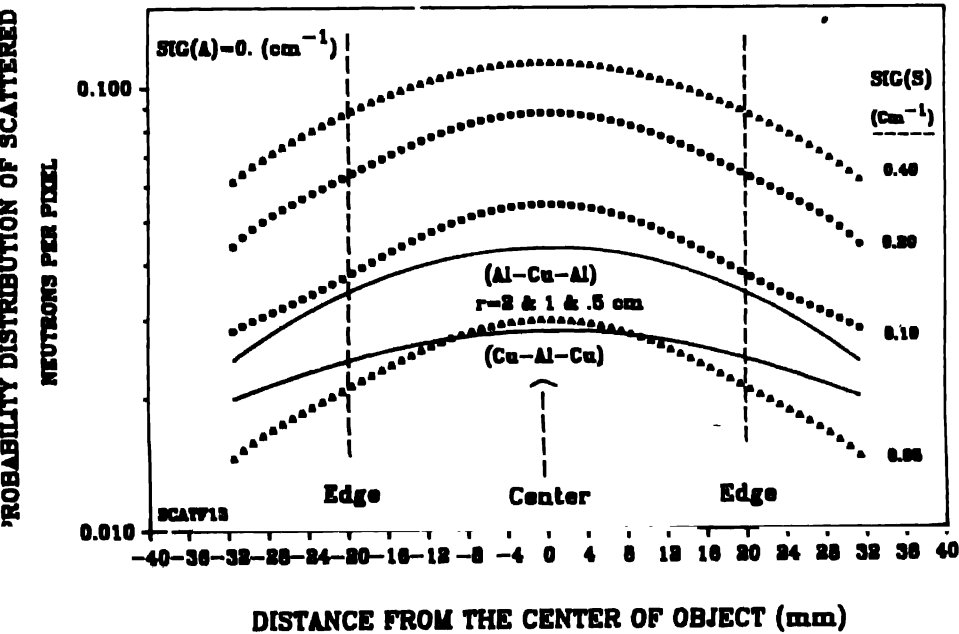


Figure 10b. The same as Figure 7, but for symmetrical samples, except Al-Cu-Al and Cu-Al-Cu replaced Al-Cu.

the middle of the detection area. This becomes quite evident when $\Sigma\alpha$ exceeds 2 cm^{-1} , thereby the probability distribution approaches zero at the middle of detection area.

For asymmetrical samples as presented in Figure 7 through 9, some discrepancies between the two cases of 0 and 180 degrees are noticed. The discrepancies are about 1 to 3 percent of the initial beam intensity, which are not detectable through our experimental work. This is due to the inaccuracies of the equipment used in the experiment. As an example, one can mention the reactor power fluctuation during the long exposure time required for producing a reliable radiograph. Moreover, the indicator level of the optical densitometer was only able to read two digits after the decimal point. Likewise, deviation from the best condition needed for film processing could be mentioned as another factor.

In order to discount the effect of the scattered neutrons, one can measure the experimental slope of the neutron scattering distribution curves and compare them with the slope of the best obtained computational curves. Through comparison, one can improve the experimental extracted data and consequently the tomographic image quality of the specimen in question.

References

- [1] H Berger *Neutron Radiography and gaging (ASTM)* (1975)
- [2] P V Der Hardt and H Rottger *Neutron Radiography Hand Book* (USA : D. Reidel) (1981)
- [3] *Neutron Radiography Proc. of the First World Conf* (San Diego, USA) (1981)
- [4] *Neutron Radiography Proc. of the 2nd World Conf* (Paris, France) (1986)
- [5] *Neutron Radiography Proc. of the 3rd World Conf* (Osaka, Japan) (1989)
- [6] R A Brooks and G D Chiro *Radiology* **177** 561 (1975)
- [7] R A Brooks and G D Chiro *Phys. Med. Biol.* **21** 639 (1976)
- [8] J A Sorenson and M E Phelps *Physics in Medicine Chap. 19* (1987)
- [9] K Kamali Moghaddam, Z Tabatabaian and N Mirhabibi *Proc. of 2nd World Conf. on Neutron Radiography* (Paris, France) p 25 (1986)
- [10] A Rosenfeld and A C Kak *Digital Picture Processing 2nd edn Vol. 1* (New York Academic) (1982)
- [11] T S Carry and J E Dowdey and Murry Christensen's *Introduction to the Physics of Diagnostic Radiology* 3rd ed (Philadelphia : Lea & Febiger) (1984)